Published in final edited form as:
Neuron. 2011 May 26; 70(4): 742–757. doi:10.1016/j.neuron.2011.04.002.

CYY-1/Cyclin Y and CDK-5 Differentially Regulate Synapse Elimination and Formation for Rewiring Neural Circuits

Mikyoung Park[1,6], **Shigeki Watanabe**[2], **Vivian Yi Nuo Poon**[3], **Chan-Yen Ou**[4], **Erik M. Jorgensen**[2], and **Kang Shen**[1,3,4,5,*]

[1]Department of Biology, Stanford University, Stanford, CA 94305, USA

[2]Department of Biology, Howard Hughes Medical Institute, University of Utah, Salt Lake City, UT 84112-0840, USA

[3]Neuroscience Program, Stanford University, Stanford, CA 94305, USA

[4]Howard Hughes Medical Institute, Stanford University, Stanford, CA 94305, USA

[5]Deparment of Pathology, Stanford University, Stanford, CA 94305, USA

Summary

The assembly and maturation of neural circuits require a delicate balance between synapse formation and elimination. The cellular and molecular mechanisms that coordinate synaptogenesis and synapse elimination are poorly understood. In *C. elegans*, DD motoneurons respecify their synaptic connectivity during development by completely eliminating existing synapses and forming new synapses without changing cell morphology. Using loss- and gain-of-function genetic approaches, we demonstrate that CYY-1, a novel cyclin box-containing protein, drives synapse removal in this process. In addition, cyclin-dependent kinase-5 (CDK-5) facilitates new synapse formation by regulating the transport of synaptic vesicles to the sites of synaptogenesis. Furthermore, we show that coordinated activation of UNC-104/Kinesin3 and Dynein are required for patterning newly formed synapses. During the remodeling process, presynaptic components from eliminated synapses are recycled to new synapses, suggesting that signaling mechanisms and molecular motors link the deconstruction of existing synapses and the assembly of new synapses during structural synaptic plasticity.

Introduction

Synapse formation and elimination are fundamental elements in both the initial construction of neural circuits and the experience-dependent modification of the mature nervous system (Sanes and Lichtman, 1999; Trachtenberg et al., 2002). During development, refinement of neural connectivity after axon guidance and dendrite morphogenesis are characterized by dynamic, regulated synaptogenesis and synapse elimination (Cline, 2001; Hua and Smith, 2004). Even in mature animals, a certain amount of “synapse turnover” is maintained,

*Corresponding Author: Kang Shen, Ph.D., Howard Hughes Medical Institute, Department of Biology, Department of Pathology, 385 Serra Mall, Herrin Labs, Stanford University, Stanford, CA 94305-5020, USA, Tel: (650)724-4255, Fax: (650)725-4309, kangshen@stanford.edu.

[6]Present Address: Center for Functional Connectomics, Korea Institute of Science and Technology, Seoul, South Korea 136-791

suggesting a balanced synapse formation and elimination is likely required for the maintenance of circuit functions. It is generally believed that neuronal activity drives the modification of neural circuits through strengthening and weakening connectivity between neurons (Balice-Gordon and Lichtman, 1994; Goda and Davis, 2003). Although a large body of work has focused on the molecular mechanisms of synapse formation, less is known about the process of synapse elimination. Very few studies have focused on the mechanisms that coordinate synaptogenesis and synapse elimination. Since synapse formation and elimination are opposite events that often take place simultaneously in the same neuron, intracellular mechanisms must exist to restrict disassembly of existing synapses and construction of new ones to distinct subcellular domains.

In *C. elegans*, six GABAergic DD motoneurons stereotypically rewire synaptic connections during larval development by eliminating existing synapses and forming new synapses without axonal or dendritic pruning. During the embryonic and the early L1 (the first larval) stages, the DD motoneurons receive synaptic inputs from cholinergic DA and DB neurons on their dorsal processes and send synaptic outputs to the ventral body muscles. At the end of the L1 stage, the DD motoneurons completely disassemble and eliminate their presynaptic terminals from the ventral processes and form new synapses on the dorsal processes (White et al., 1978; Hallam and Jin, 1998). Consequently, starting from the L2 (the second larval) stage, the DD motoneurons receive synaptic inputs from cholinergic VA and VB neurons on the ventral side and send synaptic outputs to the dorsal body muscles (White et al., 1978). This dramatic and stereotyped synaptic remodeling provides us with a genetic system to study the molecular basis of structural plasticity of synaptic circuits.

The molecular mechanisms of DD synaptic remodeling are largely unknown. *lin-14*, a heterochronic gene that controls the temporal order of a variety of cell lineages, regulates the timing of DD synaptic remodeling (Hallam and Jin, 1998).

Cyclin-dependent kinase-5 (CDK-5) is a postmitotic CDK that functions exclusively in the brain and is activated by non-cyclin activators, p35 and p39 (Cheung and Ip, 2007; also see Zhang and Herrup, 2008). CDK-5 plays multiple roles in various aspects of nervous system development including neuronal migration, neuronal survival, dendritic spine formation, synaptogenesis, adult neurogenesis, neurotransmission, homeostatic plasticity, and learning and memory (Cheung et al., 2006; Cheung and Ip, 2007; Lagace et al., 2008; Seeburg et al., 2008; Lai and Ip, 2009). Transient CDK-5 activation leads to increased number of synapses in the hippocampus (Fischer et al., 2005). In addition, we found that CDK-5 and its activator, p35, critically regulate trafficking of presynaptic components to axons. We have also identified an additional pathway involving a novel cyclin, CYY-1, that functions in parallel with the CDK-5 pathway to regulate distribution of presynaptic material (Ou et al., 2010).

In this study, we investigated how CYY-1 and CDK-5 regulate synapse elimination and synapse formation during the rewiring of the DD synaptic connectivity *in vivo*. We found that CYY-1 contributes to synapse elimination by disassembling the ventral synapses, while CDK-5 contributes to synapse formation by transporting disassembled synaptic material to the new synaptic sites. We also demonstrated that synaptic components from the disassembled synapses are recycled for the formation of new synapses during synaptic remodeling. In addition, CDK-5 facilitates UNC-104/Kinesin3-mediated formation of new dorsal synapses during DD remodeling.

Results

Synaptic Remodeling Visualized by GFP::RAB-3

To directly visualize the DD synaptic remodeling process, including synapse elimination and synapse formation, we labeled DD presynapses by expressing GFP::RAB-3 (Mahoney et al., 2006; Klassen and Shen, 2007) under the DD-specific *flp-13* promoter (Kim and Li, 2004). In synchronized cultures, the distribution of RAB-3 fluorescence in the dorsal and ventral processes of DD neurons was examined at various time points including 11, 16, 18, 19.5, 22, 26, and 28-hrs after egg-laying (Figure S1). A cytoplasmic mCHERRY marker was used to accurately identify the DD processes. Before synaptic remodeling, all GFP::RAB-3 puncta are located ventrally (Figure S1, B1). Upon the start of remodeling, ventral puncta gradually become smaller (Figure S1, B2, B3), weaker (Figure S1, B4), and eventually disappear (Figure S1, B5). Concurrently, RAB-3 puncta appear in the dorsal processes and become more intense over time (Figure S1, B3–B5). DD synaptic remodeling process was quantified by counting animals containing GFP::RAB-3 puncta only in the ventral processes (only V), both in ventral and dorsal processes (V+D), or only in the dorsal processes (only D) as shown in Figure S1C. Indeed, we observed a steady decrease in "only V" animals and a concomitant increase in the "only D" animals throughout the remodeling process, indicative of the gradual elimination of ventral synapses and the concurrent formation of dorsal synapses (Figure S1C). We chose to focus the present study on the time points 16, 18, 19.5, 22, and 26-hr after egg-laying during which the majority of the remodeling process takes place (Figure S1C).

Involvement of CYY-1 and CDK-5 in DD Synaptic Remodeling

We have recently identified that a novel protein, CYY-1, which contains a cyclin-like domain, and CDK-5 are important for the correct localization of presynaptic components in *C. elegans* (Ou et al., 2010). Since the remodeling of DD synapses involves the formation of new synapses in distal axons, it is likely that regulation of axonal transport is an important step during this structural plasticity process. Therefore, we tested if these two molecules, CYY-1 and CDK-5 affect synaptic remodeling of DD neurons.

To do this, we utilized the putative null alleles *cyy-1 (wy302)* and *cdk-5 (ok626)*. In L1-staged *cyy-1* or *cdk-5* animals, RAB-3 fluorescence is distributed only in the ventral process (Figure 1, A3 and A5) just as in *wild-type* animals (Figure 1, A1). However, in the L4 or young adult-staged *cyy-1* or *cdk-5* animals, RAB-3 fluorescence still remains in the ventral process (Figure 1, A4 and A6) unlike in the *wild-type* controls, where RAB-3 is only found in the dorsal processes (Figure 1, A2). Furthermore, in *cyy-1 cdk-5* double-mutants, while the RAB-3 fluorescence is only found in the ventral process in L1 animals (Figure 1, A7) just as in the *wild-type* controls (Figure 1, A1), the majority of the RAB-3 fluorescence remains in the ventral process in L4 or young adult animals, indicative of near complete failure of DD remodeling (Figure 1, A8). Other synaptic vesicle proteins, SNB-1/synaptobrivin and SNG-1/synaptogyrin, also showed a similar phenotype to RAB-3 in *cyy-1 cdk-5* double-mutants (Figure S2). These results suggest that CYY-1 and CDK-5 are not required for patterning of synapses in the L1 stage, but they are essential for DD synaptic remodeling.

Because that other synaptic vesicle proteins SNB-1/synaptobrivin and SNG-1/synaptogyrin, displayed a similar phenotype to RAB-3 in the double-mutants (Figure S2) and that GFP::RAB-3 reliably visualized DD synaptic remodeling process (Figure S1), we used GFP::RAB-3 (*wyIs202*) for further experiments to label synaptic vesicles during the DD remodeling process.

To ensure that the GFP::RAB-3 phenotype in the mutants indeed represents synaptic remodeling defects, we co-labeled synaptic vesicles and active zones with RAB-3 and SYD-2/Liprin-α, respectively. In the *cyy-1 cdk-5* double-mutants, SYD-2 exhibited a similar phenotype as synaptic vesicle proteins–the majority of SYD-2 signals were found in the ventral process, which colocalize with the RAB-3 puncta in the ventral process at the L4 stage (Figure 1B).

Furthermore, we performed serial electron microscopy reconstruction (EM) to definitively examine the synaptic structural defects in the double mutants. We reconstructed dorsal nerve cord and analyzed the appearance of synaptic vesicles and active zones of DD neurons in *wild-type* and *cyy-1 cdk-5* double-mutant worms. Consistent with the results from the fluorophore-tagged synaptic markers (Figures 1A, 1B, and S2), the number of synaptic vesicles and active zones in the DD dorsal process is significantly reduced in the adult double-mutant worms (Figure 1C–1E). Taken together, our findings suggest that CYY-1 and CDK-5 combined, are necessary for eliminating presynapses from the ventral process and forming new synapses in the dorsal process of DD neurons.

CYY-1 and CDK-5 Trigger DD Synaptic Remodeling

Since both CYY-1 and CDK-5 are necessary for the completion of synaptic remodeling, we next tested if these two proteins are sufficient to initiate DD synaptic remodeling. In adult *cyy-1 cdk-5* double-mutants, the majority of the GFP::RAB-3 remains in the ventral processes, suggesting that the DD synaptic remodeling is almost completely blocked in the absence of these two molecules (Figure S3, B1, quantified in Figure S3C). To ask whether CYY-1 and CDK-5 play instructive roles in the remodeling process, we tested if expression of CYY-1 and CDK-5 at the mid-L3 stage, a time point long after the normal remodeling process has been completed in *wild-type* worms, can rescue the remodeling defect in *cyy-1 cdk-5* double-mutant animals (Figure S3A). To induce CYY-1 and CDK-5 expression, we generated transgenic worms expressing CYY-1 and CDK-5 under the control of the heat-shock promoter (*Phs*). Without heat-shock treatment, *cyy-1 cdk-5*; *Ex[Phs::cyy-1, Phs::cdk-5]* worms distribute most GFP::RAB-3 puncta in the ventral processes at the young adult stage (Figure S3, B2; quantified in Figure S3C). A small amount of rescue was observed (Figure S3C) possibly due to the leaky expression of CYY-1 and CDK-5 under the heat-shock promoter. Interestingly, after heat-shock treatment (2 hrs at 30 °C), *cyy-1 cdk-5; Ex[Phs::cyy-1, Phs::cdk-5]* worms showed a dramatic rescue of the DD synaptic remodeling defect, indicated by the disappearance of ventral GFP::RAB-3 puncta as well as the appearance of dorsal GFP::RAB-3 puncta (Figure S3, B4; quantified in Figure S3C). As a control, in *cyy-1 cdk-5* double-mutants without the transgene, DD synaptic remodeling is still blocked after heat-shock treatment (Figure S3, B3; quantified in Figure S3C). In addition, heat-shock treatment at the L4 stage also achieved a significant rescue of the DD synaptic remodeling defect in the double-mutants (data not shown), indicating that the expression of these molecules can drive the remodeling process. Taken together, these data argue that expression of CYY-1 and CDK-5 is sufficient to trigger the synaptic remodeling process even at very late stages of development. In other words, the remodeling process was suspended in the double mutants, but could still proceed when CYY-1 and CDK-5 were expressed later in life.

CYY-1 Functions in Ventral Presynapse RAB-3 Elimination During DD Synaptic Remodeling

To further dissect CYY-1's role during DD remodeling, we analyzed the loss-of-function phenotype of *cyy-1(wy302)* mutants at different time points during the remodeling process. In addition to counting the "only V", "V+D" and "only D" worms within a population (Figure 2D), we also measured the average fluorescence intensity of ventral (Figure 2F) and

dorsal RAB-3 puncta (Figure 2G). The *cyy-1* worm exhibits significant amounts of punctuate ventral GFP::RAB-3 even at the late remodeling time points of 22- and 26-hr after egg-laying compared to *wild-type* (Figure 2B, V inserts; quantified in Figure 2F) with only slight reduction of the amount of dorsal GFP::RAB-3 at 26-hr time point compared to *wild-type* (Figure 2G). In addition, *cyy-1* mutants have a reduced percentage of worms displaying complete remodeling (Figure 2D, green-lined black-filled at 26-hr) compared to *wild-type* worms (Figure 2D, red-lined black-filled at 26-hr). These data suggest that CYY-1 is involved in GFP::RAB-3 elimination during the remodeling process.

If CYY-1 is a critical molecule to instruct the synapse elimination process, manipulation of CYY-1 expression might lead to precocious elimination of synapses from the ventral processes. To test this hypothesis, we expressed CYY-1 in DD neurons using the DD-specific *flp-13* promoter whose expression is initiated in embryos, well before the normal developmental time for the remodeling process. Indeed, overexpression of CYY-1 increases the percentage of worms showing GFP::RAB-3 signals in both ventral and dorsal processes (V+D) at the 16-hr time point (Figure 2D, yellow-lined gray-filled) and also increases the ratio of dorsal to ventral plus dorsal [D/(V+D)] GFP::RAB-3 intensity (Figure 2E), which are indicative of accelerated remodeling.

Delayed ventral GFP::RAB-3 elimination in *cyy-1* mutants (Figure 2D, green-lined black-filled) was rescued by specific expression of CYY-1 in DDs (Figure 2D, purple-lined black-filled). These results indicate that CYY-1 acts cell-autonomously in DDs. Taken together, the delayed GFP::RAB-3 elimination in the *cyy-1* mutants and the accelerated GFP::RAB-3 elimination in CYY-1-overexpressing animals argue that CYY-1 is required for the elimination of existing GFP::RAB-3 presynaptic structures in the ventral process.

Consistent with our finding of CYY-1 in ventral GFP::RAB-3 elimination during DD synaptic remodeling, distribution of CYY-1 in DDs shifts to ventral from dorsal processes during the remodeling (Figure S4), further supporting its role in ventral synapses.

CDK-5 Facilitates the Formation of New Dorsal RAB-3 Puncta for DD Synaptic Remodeling

Interestingly, careful inspection of *cdk-5* and *cyy-1* loss- and gain-of-function of animals revealed both similarities and differences in their DD remodeling phenotypes. Specifically, in *cdk-5* mutants, formation of new dorsal GFP::RAB-3 is significantly delayed compared to *wild-type* worms (Figure 3B, D inserts of B4–B6 compared to those of B1–B3; Figure 3D, green-lined gray-filled compared to red-lined gray-filled; quantified in Figure 3G). Moreover, by 26 hours, none of *cdk-5* mutants show completed remodeling (Figure 3D, green-lined gray-filled at 26-hr; quantified in Figure 3F), suggesting that similar to CYY-1, CDK-5 is also required for the completion of the remodeling process.

To determine whether CYY-1 and CDK-5 play similar roles in DD remodeling, we performed gain-of-function experiments by overexpressing CDK-5 in DD neurons of *wild-type* worms. Transgenic worms overexpressing CDK-5 show accelerated remodeling at the early time points 16- and 18-hr after egg-laying compared to *wild-type* (Figure 3E; Figure 3C, D insert of C4 compared to that of C1; Figure 3D, yellow-lined gray-filled compared to red-lined gray-filled; quantified in Figure 3G).

Interestingly, the intensity of ventral GFP::RAB-3 was not affected in worms overexpressing CDK-5 (Figure 3F), implying that, unlike CYY-1, CDK-5 is probably not directly involved in the elimination of ventral GFP::RAB-3. Instead, CDK-5 appears to affect the clearance of RAB-3 through other mechanisms. The remodeling phenotype in *cdk-5* mutants (Figure 3D, green) was rescued by overexpressing CDK-5 in DD neurons (Figure 3D, purple), indicating that CDK-5 acts cell-autonomously in DD neurons.

CYY-1 and CDK-5 Differentially Regulate Synapse Elimination and Formation During DD Synaptic Remodeling

The above mentioned data suggest that although both CYY-1 and CDK-5 are required for DD synaptic remodeling, their specific functions might be different. Our data indicate that CYY-1 promotes the removal of ventral GFP::RAB-3 puncta while CDK-5 promotes the assembly of dorsal GFP::RAB-3 puncta. To further test this model, we investigated the epistatic relationship between these two genes. We first tested whether overexpression of CYY-1 in the *cdk-5* single-mutant background can substitute for the lack of CDK-5 function. If CYY-1 and CDK-5 play different roles in DD remodeling, overexpression of CYY-1 in the *cdk-5* single-mutant should not rescue the *cdk-5* mutant phenotype; furthermore, CYY-1 overexpression in the *cdk-5* mutant background might cause the removal of ventral GFP::RAB-3. Consistent with these predictions, overexpression of CYY-1 does not rescue the delayed and incomplete remodeling in the *cdk-5* mutants (Figure 4, A4; Figure 4B, purple-lined gray-filled; Figure 4C) compared to *cdk-5* without the transgene (Figure 4A, A3; Figure 4B, green-lined gray-filled; Figure 4C). The CYY-1 transgene is functional since it rescues the *cyy-1* mutant phenotype (Figure 2D). In addition, overexpressing CYY-1 still caused the elimination of ventral GFP::RAB-3 even in the *cdk-5* mutant background (Figure 4A, A4; quantified in Figure 4D), again supporting the model that the function of CYY-1 to remove RAB-3 in the ventral process is independent of CDK-5.

The accelerated new synapse formation caused by the CYY-1 overexpression (Figure 2, C4; Figures 2D and 4B, yellow at 16-hr time point), however, was blocked by the *cdk-5* mutation (Figure 4B, purple; quantified in Figures 4C and 4E), suggesting that new GFP::RAB-3 puncta caused by CYY-1 overexpression does require the function of CDK-5. Taken together, these data strongly support the distinct differential roles of CYY-1 and CDK-5 during the synaptic remodeling. One possible model is that CYY-1 is required for the dispersal of existing GFP::RAB-3 structures and CDK-5 is required for transportation of the dispersed GFP::RAB-3 signals to the dorsal locations for new synapses or local assembly of new GFP::RAB-3 in the dorsal axon.

Several predictions can be made based on this model. First, if CYY-1 and CDK-5 have distinct functions, overexpression of CDK-5 should not rescue the *cyy-1* mutant phenotype. Second, if the dispersal of ventral GFP::RAB-3 signals from the ventral synapses precedes the formation of new synapses, slowing down synapse elimination should hamper the formation of new synapses. Third, if the dispersal of synaptic material from the existing synapses is reused for the formation of new synapses, one should be able to observe that directly by marking disassembled synaptic material. To test these predictions, we performed the following experiments.

First, we overexpressed CDK-5 in the *cyy-1* single-mutant background, and found that the incomplete remodeling in the *cyy-1* mutant was not rescued by the CDK-5 transgene (Figure 5B, purple compared to green). Second, the accelerated dorsal formation of GFP::RAB-3 puncta caused by overexpression of CDK-5 is blocked by the *cyy-1* mutation (Figure 5A, A4 compared to A2; Figure 5B, yellow compared with purple; quantified in Figures 5C–5E), suggesting that the function of CYY-1 might proceed the action of CDK-5 during the remodeling. Thus, it is conceivable that CYY-1 disassembles ventral synapses, from which the materials are then transported to dorsal processes and recycled for new synaptogenesis events.

Disassembled Ventral Synaptic Material Is Reused for Dorsal Synapse Formation During DD Synaptic Remodeling

To definitively test if synapse disassembly is a prerequisite step that contributes to dorsal synapse formation, we directly visualized the fate of ventral RAB-3 molecules during DD remodeling using a photoswitchable GFP (Dendra2) whose fluorescence is irreversibly converted from green to red by UV irradiation (Ando et al., 2002; Arimura et al., 2004; Miyawaki, 2004; Gurskaya et al., 2006). In these photocoversion experiments, we selected Dendra2::RAB-3-expressing worms (Figure 5, F1) around the 16–18-hr time point. Local UV irradiation of the DD2 ventral process resulted in immediate photoconversion from green to red fluorescence in worms expressing Dendra2::RAB-3 (Figure 5, F2). Then, we tracked the red fluorescence to determine if the red RAB-3 molecules are eventually clustered at the newly formed dorsal synapses. Indeed, we found that 8–10 hrs after UV irradiation, clustered Dendra2::RAB-3 red fluorescence was found in the dorsal process (Figure 5, F4; quantified in Figure 5G). As a control, DD1 neuron that has not been activated by UV did not show any red fluorescence of Dendra2::RAB-3 (Figure 5, F4) but showed the green fluorescence as DD2 neuron (Figure 5, F3). These results suggest that ventral synaptic vesicle protein RAB-3 is transported to dorsal processes to form new synapses during DD synaptic remodeling.

These observations are consistent with the model that CYY-1 is responsible for the dispersal of ventral RAB-3 puncta while CDK-5 promotes the transport of the ventral GFP::RAB-3 and the formation of new RAB-3 puncta in the dorsal process. To further test this model, we performed the same photoconversion experiment in *cyy-1* and *cdk-5* mutants. If CYY-1 regulates ventral RAB-3 elimination and CDK-5 regulates the transportation of the ventral RAB-3 to the dorsal side, then the percentage of photoconverted red signal in dorsal synapses should be significantly lower in *cyy-1* and *cdk-5* mutants. As expected, we found that the percentages of photoconverted red signal in the dorsal process are significantly lower in *cyy-1* (38.6 %) and *cdk-5* (8.4 %) mutants than in *wild-type* (59.5 %) worms (Figure 5G). In particular, the percentage of photoconverted red signal that is remained in the ventral process is much higher in *cyy-1* (56.4 %) and *cdk-5* (30.3 %) mutants than in *wild-type* (6.2 %) worms (Figure 5G), likely due to the blockade of elimination of RAB-3 proteins in *cyy-1* and the blockade of transportation of RAB-3 from the ventral to the dorsal process in *cdk-5* mutants, respectively. In addition, a combined 95% (ventral 56.4 % + dorsal 38.6 %) of photoconverted RAB-3 remain at 8–10 hr after UV in *cyy-1* mutants compared with 65.7% (ventral 6.2 % + dorsal 59.5 %) in *wild-type* worms, indicating the blockade of the elimination of RAB-3 proteins in *cyy-1* mutants.

Taken together, these data strengthen our model that CYY-1 mediates the elimination of ventral RAB-3 proteins, while CDK-5 mediates the transportation of ventral RAB-3 proteins to the dorsal process to form new synapses during DD remodeling.

Remnant Ventral RAB-3 Puncta in *cyy-1*, But Not in *cdk-5* Mutants Represent Presynaptic and Postsynaptic Specializations

Our model indicates that the ectopic ventral GFP::RAB-3 puncta in *cyy-1* resulted from the failure of synapse elimination, while those in *cdk-5* resulted from the failure of the transportation of the disassembled ventral GFP::RAB-3 to the dorsal side. Therefore, it predicts that the ectopic ventral GFP::RAB-3 in *cyy-1*, but not in *cdk-5*, might represent functional presynaptic and postsynaptic specializations. To test this, we first examined whether the ectopic ventral GFP::RAB-3 puncta in *cyy-1* or *cdk-5* colocalize with an active zone protein SYD-2. Consistent with our prediction, the ectopic ventral GFP::RAB-3 in *cyy-1*, but not in *cdk-5* mutants shows a high degree of colocalization with

mCHERRY::SYD-2 (Figures 6A and 6B). These results indicate that the ectopic RAB-3 puncta in *cyy-1*, but not *cdk-5* mutants might represent presynaptic specializations.

To further address the functionality of GFP::RAB-3 puncta, we tested if the ventral GFP::RAB-3 labeled synaptic vesicles in *cyy-1*, but not *cdk-5* mutants, undergo exocytosis. Mutations in *unc-13* genes has been reported to have defects in the exocytosis of synaptic vesicles (Brose et al., 2000) and lead to excessive accumulations of RAB-3 at functional presynaptic terminals (Ch'ng et al., 2008). It is conceivable that such effect of *unc-13* mutants would not occur in nonfunctional presynaptic sites. Consistently, we found that the *unc-13(e450)* mutation causes increased intensity of GFP::RAB-3 puncta in DD neurons compared to *wild-type* background (data not shown). We next generated *unc-13; cyy-1* and *unc-13; cdk-5* double-mutants. The ventral GFP::RAB-3 puncta in *unc-13; cyy-1* double-mutants are brighter compared to *cyy-1* alone (Figures S5A and S5B), implying that the ventral GFP::RAB-3 puncta in *cyy-1* single-mutants might represent functional presynaptic specializations. However, the ventral GFP::RAB-3 puncta in *unc-13; cdk-5* double-mutants show similar intensity compared to *cdk-5* alone (Figures S5C and S5D), indicating that the ventral GFP::RAB-3 puncta in *cdk-5* single-mutants are not likely functional presynapses. As internal controls, dorsal GFP::RAB-3 puncta both in *unc-13; cyy-1* and *unc-13; cdk-5* double-mutants are brighter compared to *cyy-1* and *cdk-5* alone, respectively (Figure S5).

To further clarify the identities of ectopic RAB-3 puncta in *cyy-1* and *cdk-5*, we asked whether the ectopic puncta are associated with postsynaptic specializations. In *wild-type* animals, the GABAergic presynaptic SNB-1/synaptobrevin from the DD and VD neurons juxtaposes postsynaptic UNC-49/GABA receptors in the dorsal and ventral cord, respectively (Gally and Bessereau, 2003). A *lin-6* mutation that was shown to eliminate the VD neurons (Hallam and Jin, 1998) facilitates our analysis of the DD ectopic RAB-3 puncta in the ventral side of the animal. We found that ectopic ventral presynaptic SNB-1/Synaptobrevin puncta in *cyy-1*, but not *cdk-5* mutants exhibit a high degree of colocalization with postsynaptic UNC-49/GABA receptors (Figures 6C and 6D). Taken together, these data indicate that CYY-1, but not CDK-5, plays a role in synaptic vesicle elimination from synaptic sites, and strongly support the differential functions of CYY-1 and CDK-5 in synapse elimination and new synapse formation, respectively.

CDK-5 and UNC-104/Kinesin3 Act Together to Transport Synaptic Components to the New Dorsal Synaptic Sites During DD Synaptic Remodeling

To further understand how synaptic material is transported to the dorsal axon during DD remodeling, we examined the role of UNC-104/Kinesin3, a kinesin motor, in this process. UNC-104 is a well-known motor protein required for axonal transport (Hall and Hedgecock, 1991; Bloom, 2001; Klopfenstein and Vale, 2004; Pack-Chung et al., 2007; Niwa et al., 2008). To test if UNC-104/Kinesin3 is required for remodeling of DD synapses, we examined the remodeling process in *unc-104(e1265)* mutants. Interestingly, in L1-staged animals before remodeling (16-hr), GFP::RAB-3 localizes to the ventral process in *unc-104(e1265)* mutants (Figure S6, A1), similar as in the *wild-type* worms. However, this distribution pattern remains unchanged during the remodeling time points (Figure S6, A1–A3), and no dorsal puncta were ever observed in L2 or older animals, suggesting that the remodeling process completely fails in the *unc-104(e1265)* mutants.

We next tested if overexpressing UNC-104/Kinesin3 accelerates the remodeling process. Indeed, almost all worms overexpressing UNC-104/Kinesin3 exhibit accelerated accumulation of dorsal GFP::RAB-3 puncta (Figure 7A, D inserts of A4–A6; Figure 7C, yellow-lined gray-filled), a phenotype similar to that seen in the transgenic worms overexpressing CDK-5 (Figure 3D, yellow-lined gray-filled). The similarity of loss- and

gain-of-function phenotypes between *cdk-5* and *unc-104* suggests that CDK-5 and UNC-104 affect similar aspects of the remodeling process.

To further understand the relationship between CDK-5 and UNC-104, we overexpressed UNC-104 in the *cdk-5* mutant background. We found that UNC-104 overexpression significantly rescues the *cdk-5* mutant remodeling phenotype at all time points, suggesting that UNC-104 might function downstream of or in parallel to CDK-5 (Figure 7C, purple compared to green). In order to determine if the overexpression of UNC-104 completely bypasses the requirement for CDK-5, we compared the intensity of the dorsal RAB-3 fluorescence in *Ex[DD::UNC-104] cdk-5(+)* and *Ex[DD::UNC-104] cdk-5(−)* animals. Although dorsal GFP::RAB-3 puncta were apparent in both genetic backgrounds, it appeared that the intensity of the new dorsal GFP::RAB-3 puncta was dramatically lower in the *cdk-5(−)* background, indicating that CDK-5 facilitates the activity of UNC-104 (Figure 7A, compare D inserts of A7 and A8 to those of A4 and A5; quantified in Figure 7B). Consistent with our model, the intensity of new dorsal GFP::RAB-3 puncta in *Ex[DD::UNC-104] cyy-1(−)* animals did not exhibit significant difference (average intensity of dorsal GFP::RAB-3, normalized; 1.1 ± 0.12, n=15) compared to *Ex[DD::UNC-104] cyy-1(+)* animals (average intensity of dorsal GFP::RAB-3, normalized; 1.0 ± 0.06, n=26). We found that during DD remodeling, fluorescently-tagged CDK-5 and UNC-104 both exhibit punctate localization patterns and colocalize in the ventral and dorsal processes (Figure S6, C) as well as the commissures (Figure S6, D). Furthermore, when we overexpressed CDK-5 in the *unc-104(e1265)* background, all GFP::RAB-3 was located in the ventral processes and cell bodies (Figure S6, A4–A6), just as in the *unc-104(e1265)* single-mutant (Figure S6, A1–A3). Again, these data support the model that UNC-104 is an essential motor protein needed for the transport of synaptic material to the dorsal processes and that CDK-5 facilitates the UNC-104-mediated transport of synaptic components to the dorsal sites of new synapse formation.

UNC-104 and Dynein Motors Act Sequentially to Properly Localize Synaptic Vesicles Along the Dorsal Process In DD Synaptic Remodeling

When we closely examined the localization of GFP::RAB-3 in the dorsal process, we uncovered an intriguing interplay between the anterograde and retrograde motors during this remodeling event. We found that in 27% of the *wild-type* worms, GFP::RAB-3 fluorescence first accumulated at the most distal ends of the DD neurons at around the 20–22-hr time points (Figure 8A, upper image; Figure 8E). Subsequently, fluorescence became evenly redistributed along the dorsal processes at around the 26-hr time point (Figure 8A, lower image), suggestive of a two-step trafficking process during DD remodeling: (1) early anterograde trafficking of synaptic vesicles from the ventral process all the way to the anterior and posterior ends of the dorsal process and (2) late retrograde movement that results in the even distribution pattern of synaptic vesicles along the dorsal process.

Interestingly, we found that overexpression of UNC-104 led to dramatic, fully penetrant accumulation of GFP::RAB-3 at the distal ends of the dorsal process even at the 26-hr time point (Figures 8B, 8E, and 8F), while loss-of-function mutants of UNC-104 showed a complete block of dorsal delivery of GFP::RAB-3 (Figure 8C).

As shown in Figure 8A, the accumulation of GFP::RAB-3 at both ends is transient and fluorescence was then redistributed along the entire dorsal axon in a punctate pattern, similar to the pattern observed in adult animals. Because an anterograde motor UNC-104 directs GFP::RAB-3 to both ends of the dorsal processes, we hypothesized that a retrograde motor Dynein might be responsible for the redistribution of GFP::RAB-3 by delivering the end accumulated GFP::RAB-3 toward the opposite direction to UNC-104.

To test this hypothesis, we disrupted the function of Dynein using a loss-of-function allele of *dynein, dhc-1(js319)*, which has been shown to result in an accumulation of SNB-1/synaptobrevin at the tips of mechanosensory neuronal processes (Koushika et al., 2004). Indeed, more than 50% of the *dhc-1* mutants accumulated GFP::RAB-3 proteins in the distal ends of dorsal processes during remodeling (Figures 8D and 8F). This end accumulation phenotype of GFP::RAB-3 in *dhc-1* mutants is inhibited in *dhc-1; cdk-5*, but not in *dhc-1; cyy-1* double-mutants (Figure 8F), indicating that CDK-5, but not CYY-1 contributes to the end accumulation of GFP::RAB-3. These data further support that CDK-5 and UNC-104 act together in the process of new dorsal synapse formation during DD remodeling. Taken together, we propose that two different microtubule motors interplay temporally for proper localization of new synapses during the remodeling process (Figure 8G).

Discussion

In the present study, our data showed that destruction of existing synapse is regulated by a cyclin box-containing protein CYY-1. The disassembled synaptic components are then transported to the dorsal processes of DDs by an axonal transport motor UNC-104/Kinesin3. In the absence of CDK-5, dorsal synapse formation during remodeling is significantly delayed, possibly also due to insufficient activation of UNC-104/Kinesin3-mediated axonal transport. Once CDK-5 and UNC-104/Kinesin3 bring the synaptic components to the dorsal axon through the commissure, the synaptic components are finally positioned at the proper synaptic locations by dynein complexes (Figure S7).

Concurrent Synapse Elimination and New Synapse Formation During DD Remodeling

The stereotyped reversal of synaptic connectivity of DD motoneurons during *C. elegans* development has long been considered as an attractive model system to study synaptic plasticity (White et al., 1978; Hallam and Jin, 1998). While it has been well established that the ventral synapses in the L1 animal are eventually eliminated and the new synapses are formed in the dorsal axon, the relationship between synapse formation and elimination has not been well understood. By specifically labeling the presynaptic terminals of the DD neurons and performing time course experiments, we have been able to directly visualize the remodeling process *in vivo*. Interestingly, we found that the elimination of existing synapses and the formation of new synapses occur simultaneously within a certain time window during the DD remodeling process (Figure S1). This is analogous to many observations made in the vertebrate systems. For example, retinal ganglion axons form synapses with tectal neurons through a dynamic process characterized by concurrent synapse formation and elimination in the same presynaptic axon (Debski and Cline, 2002; Ruthazer et al., 2006). In the well-studied vertebrate neuromuscular junction, an initial stage of synapse formation leads to each muscle fiber being innervated by multiple motor axons, which is then followed by a period of synaptic competition, resulting in the mature monoinnervation pattern. During the activity driven competition, one of the motor axons gains its innervation while other axons loses their synaptic connections to each particular muscle fiber, suggesting that synapse formation and elimination take place concurrently in the same postsynaptic muscle (Lichtman and Colman, 2000).

Since constructing and deconstructing synapses happen simultaneously in the same cell, it is conceivable that synaptic components might be “reused” at new synapses. Indeed, our experiments provide evidence that this might be true. We specifically marked the synaptic vesicles at existing synapses, which are destined for destruction, and the labeled vesicles were later found at the new synaptic sites. These data further suggest that synapse elimination might not be a total demolition of existing synapses, but instead may be a controlled disassembly process from which synaptic vesicles and synaptic proteins can be potentially recycled for building new synapses.

CYY-1 and CDK-5 Are Key Players for Structural Plasticity in the DD Neurons

The stereotyped structural rearrangement of the DD neurons provides an opportunity to study coordinated synapse elimination and synapse formation in the same cells *in vivo*. This remodeling process is regulated by the heterochronic gene *lin-14*, which controls the timing of stage-specific cell lineages in *C. elegans* (Ambros and Horvitz, 1984, 1987; Ambros and Moss, 1994). In loss-of-function mutants of *lin-14*, DD neurons remodel precociously, suggesting that LIN-14 suppresses the initiation of the remodeling process (Hallam and Jin, 1998).

Our loss-of-function and gain-of-function genetic analyses suggest that the CYY-1 and CDK-5 are essential for the synaptic remodeling process. In either single-mutant, the DD remodeling process becomes delayed and incomplete. In double-mutants lacking both CYY-1 and CDK-5, the remodeling is almost completely blocked. Overexpression of CYY-1 and CDK-5 leads to precocious remodeling, suggesting that they are both necessary and might also instruct the initiation of remodeling. A critical experiment to distinguish the permissive and instructive nature of these genes is to ask if remodeling can be restored at a very different time during development by artificial expression of these two genes. Surprisingly, in the *cyy-1 cdk-5* double-mutants in which the synaptic remodeling is more or less completely blocked, the induced expression of both genes at mid-L3, a stage long after the endogenous remodeling time, was able to dramatically reinstate the remodeling process. This result strongly suggests that the remodeling program is halted in the double-mutants, “waiting” for the expression of CYY-1 and CDK-5. As such, CYY-1 and CDK-5 together can drive the remodeling process. It is likely that the endogenous expression or activities of these two genes are regulated during the initiation and progression of the remodeling process. It will be interesting to determine whether LIN-14 regulates the timing of remodeling through CDK-5 or CYY-1.

Regulation of Axonal Transport As Key Components in Neural Plasticity

Since synapse formation often occurs in the distal axon, far away from the cell body where many synaptic organelles and proteins are generated, it is conceivable that the transport of synaptic material to the synaptic sites can be the rate-limiting step in synapse formation. Indeed, several studies have shown that the regulation of anterograde microtubule-mediated transport is a key step in synaptic plasticity. For example, in the gill-withdrawal reflex circuit of *Aplysia*, the induction of long-term facilitation requires upregulation of kinesin heavy chain (Puthanveettil et al., 2008). In another study, the kinesin family member 5B (KIF5B) motor and its adaptor syntabulin were shown to be required for the formation of new presynaptic boutons during activity-dependent synaptic plasticity in hippocampal neurons (Cai et al., 2007).

During the remodeling of DD synaptic connectivity, we found that the anterograde motor UNC-104/Kinesin3 is absolutely required for the formation of new synapses. CDK-5 likely promotes new synapse formation by stimulating UNC-104. Intriguingly, we found that a retrograde motor, the dynein complex is also required for synapse formation. During the normal remodeling process, synaptic vesicles transiently accumulate at the terminals of DD axon, but later redistribute along the entire axon through dynein activity. In the dynein heavy chain mutants, this redistribution step is disrupted (Figure 8D). It is likely that temporal regulation of motor activity is required to generate the dynamic behavior. For example, it is conceivable that the UNC-104-mediated anterograde transport dominates in early stages of the remodeling process, driving synaptic material to the anterior and posterior ends of the dorsal DD processes. Then, at later time points, the retrograde motor is now activated which distributes the synaptic material along the entire dorsal axon. These data

suggest that both UNC-104/Kinesin3 and the dynein complex are required for the appropriate formation of new synapses during the rewiring of DD synapses.

Do CYY-1 and CDK-5 Play Different Functions in Different Neurons?

In a recent study, we reported the function of CYY-1 and CDK-5 in the DA9 neuron, which does not undergo dramatic structural rearrangement of its synapses. There are interesting similarity and difference between the phenotypes in the DDs and in the DA9 that raise the question whether these molecular pathways play similar or distinct roles in patterning synaptic material in different cell types.

The similarity is apparent. In the *cyy-1 cdk-5* double-mutants, presynaptic material, including synaptic vesicles and active zone proteins dramatically mislocalize to dendrites in both DDs and DA9. However, the mislocalization in the DD neurons results from a failure of synaptic remodeling since synaptic localization in L1 is normal. On the contrary, the DA9 mislocalization phenotype is evident as soon as its dendrite is born, arguing that CYY-1 and CDK-5 in DA9 are required at different time points (Ou et al., 2010). Despite the phenotypic similarity between the two cell types, detailed analysis reviewed three major differences. First, mutations in *dhc-1* and other constituents of the cytoplasmic dynein complex dramatically suppress the dendritic mislocalization of presynaptic components in DA9, suggesting that dynein mediated retrograde transport is a major downstream pathway for CYY-1 and CDK-5 in DA9 (Ou et al., 2010). However, the same *dhc-1* mutation only subtly suppresses the DD phenotype of the *cyy-1 cdk-5* double-mutants, suggesting that addition downstream pathways are required in the remodeling process (data not shown).

Secondly, the functions of CDK-5 appear to be different in these two cell types. Loss of *cdk-5* results in marked increase in the number of both retrograde and anterograde trafficking events in the DA9 axons, arguing that CDK-5 does not likely promote anterograde trafficking (Ou et al., 2010). On the hand, CDK-5 facilitates UNC-104 mediated anterograde traffic during the DD remodeling process. Considering the numerous target substrates of CDK-5, it is conceivable that CDK-5 also facilitates anterograde trafficking but this effect is masked by its effect in suppressing retrograde transport. Thirdly, the *cyy-1* activated PCTAIRE kinase, PCT-1 plays a more important role in DA9 than in DDs, because loss of *pct-1* alone causes a full penetrant phenotype in DA9 (Ou et al., 2010), but not in DDs (data not shown). Further understanding of the molecular downstream players in the CYY-1 and CDK-5 pathway will elucidate the similarity and differences in these two cells.

Experimental Procedures

Strains and Genetics, molecular biology, heat-shock experiment, and confocal imaging are described in the Supplemental Data.

Staging and Analysis

To precisely synchronize the worms at a stage, gravid adult worms were collected and allowed to lay eggs for 1 hour at 25 °C. Eggs were placed at 25 °C to develop for appropriate duration, mainly 11, 16, 18, 19.5, 22, and 26 hours for each experimental purpose. Then, the phenotype of DD synaptic remodeling was examined. We did not notice any obvious egg-laying abnormalities for the mutant and transgenic strains we have used for our analysis.

Local Photoconversion of Dendra2::RAB-3

L1 worms around 16–18-hr after egg-laying (i.e., before starting synaptic remodeling) were sampled under a coverslip in Levamisole (1 mM, Sigma). Worms expressing Dendra2::RAB-3 were identified by the expression of co-injection marker P*odr-1::dsred*. Dendra2::RAB-3 puncta in the DD2 ventral process were locally photoconverted using a 405-nm laser at 30 mW power for 20 seconds through 63× objective (NA 1.4). Eight to 10 hours after UV irradiation, photoconverted red fluorescent signals were examined and quantified.

Image Analysis and Quantification

To measure the average fluorescence intensity, the ventral and dorsal processes of DD neurons without the cell bodies were carefully traced and the background intensity subtracted from the intensity in the traced regions using *ImageJ*. The ratio of dorsal to ventral plus dorsal [D/(V+D)] GFP::RAB-3 was calculated by the following formula: average intensity of dorsal GFP::RAB-3/(average intensity of ventral GFP::RAB-3 + average intensity of dorsal GFP::RAB-3).

For the analysis of photoconverted experiment, the integrated intensity of photoconverted red fluorescence of RAB-3 in the ventral (V) and the dorsal (D) process at 8–10 hr after UV irradiation was normalized to the integrated intensity of photoconverted red fluorescence of RAB-3 in the ventral process right after UV irradiation. For other detailed descriptions of image analysis and quantification, see Supplemental Data.

Electron Microscopy

DD neurons were reconstructed and analyzed from N2 *wild-type* and *cyy-1 cdk-5* animals as previously described (Ou et al., 2010). DD neurons were identified by their position and orientation within the dorsal nerve cord. A varicosity was defined as a series of profiles with an area larger than 10,000 square nm regardless of the existence of dense projections. Detailed methods are provided in the Supplemental Data.

Supplementary Material

Refer to Web version on PubMed Central for supplementary material.

Acknowledgments

We thank C. Gao and Y.-Y. Fu for technical assistance. We thank the *Caenorhabditis* Genetics Center and the Japanese NBRP for strains. We thank Christopher Li for sharing the information on the sequence of the *flp-13* promoter region, and Bing Ye for reagents. We also thank Andrew Hellman, Jaewon Ko, Yulong Li, Oliver Liu, Jiuyi Lu, and Maulik Patel for critical comments on the first draft of this manuscript. This work was supported by grants NIH 5R01 NS048392, W.M. Keck Foundation, and International Human Frontier Science Program Organization (to K.S.) and the Lucile Packard Foundation for Children's Health and the American Heart Association postdoctoral fellowship (to M.P.). K.S. is an Investigator of the Howard Hughes Medical Institute.

References

Ambros V, Horvitz HR. Heterochronic mutants of the nematode Caenorhabditis elegans. Science. 1984; 226:409–416. [PubMed: 6494891]

Ambros V, Horvitz HR. The lin-14 locus of Caenorhabditis elegans controls the time of expression of specific postembryonic developmental events. Genes Dev. 1987; 1:398–414. [PubMed: 3678829]

Ambros V, Moss EG. Heterochronic genes and the temporal control of C. elegans development. Trends Genet. 1994; 10:123–127. [PubMed: 8029828]

Ando R, Hama H, Yamamoto-Hino M, Mizuno H, Miyawaki A. An optical marker based on the UV-induced green-to-red photoconversion of a fluorescent protein. Proc Natl Acad Sci U S A. 2002; 99:12651–12656. [PubMed: 12271129]

Arimura S, Yamamoto J, Aida GP, Nakazono M, Tsutsumi N. Frequent fusion and fission of plant mitochondria with unequal nucleoid distribution. Proc Natl Acad Sci U S A. 2004; 101:7805–7808. [PubMed: 15136720]

Balice-Gordon RJ, Lichtman JW. Long-term synapse loss induced by focal blockade of postsynaptic receptors. Nature. 1994; 372:519–524. [PubMed: 7990923]

Bloom GS. The UNC-104/KIF1 family of kinesins. Curr Opin Cell Biol. 2001; 13:36–40. [PubMed: 11163131]

Brose N, Rosenmund C, Rettig J. Regulation of transmitter release by Unc-13 and its homologues. Curr Opin Neurobiol. 2000; 10:303–311. [PubMed: 10851170]

Cai Q, Pan PY, Sheng ZH. Syntabulin-kinesin-1 family member 5B-mediated axonal transport contributes to activity-dependent presynaptic assembly. J Neurosci. 2007; 27:7284–7296. [PubMed: 17611281]

Ch'ng Q, Sieburth D, Kaplan JM. Profiling synaptic proteins identifies regulators of insulin secretion and lifespan. PLoS Genet. 2008; 4 e1000283.

Cheung ZH, Fu AK, Ip NY. Synaptic roles of Cdk5: implications in higher cognitive functions and neurodegenerative diseases. Neuron. 2006; 50:13–18. [PubMed: 16600851]

Cheung ZH, Ip NY. The roles of cyclin-dependent kinase 5 in dendrite and synapse development. Biotechnol J. 2007; 2:949–957. [PubMed: 17526057]

Cline HT. Dendritic arbor development and synaptogenesis. Curr Opin Neurobiol. 2001; 11:118–126. [PubMed: 11179881]

Debski EA, Cline HT. Activity-dependent mapping in the retinotectal projection. Curr Opin Neurobiol. 2002; 12:93–99. [PubMed: 11861170]

Fischer A, Sananbenesi F, Pang PT, Lu B, Tsai LH. Opposing roles of transient and prolonged expression of p25 in synaptic plasticity and hippocampus-dependent memory. Neuron. 2005; 48:825–838. [PubMed: 16337919]

Gally C, Bessereau JL. GABA is dispensable for the formation of junctional GABA receptor clusters in Caenorhabditis elegans. J Neurosci. 2003; 23:2591–2599. [PubMed: 12684444]

Goda Y, Davis GW. Mechanisms of synapse assembly and disassembly. Neuron. 2003; 40:243–264. [PubMed: 14556707]

Gurskaya NG, Verkhusha VV, Shcheglov AS, Staroverov DB, Chepurnykh TV, Fradkov AF, Lukyanov S, Lukyanov KA. Engineering of a monomeric green-to-red photoactivatable fluorescent protein induced by blue light. Nat Biotechnol. 2006; 24:461–465. [PubMed: 16550175]

Hall DH, Hedgecock EM. Kinesin-related gene unc-104 is required for axonal transport of synaptic vesicles in C. elegans. Cell. 1991; 65:837–847. [PubMed: 1710172]

Hallam SJ, Jin Y. lin-14 regulates the timing of synaptic remodelling in Caenorhabditis elegans. Nature. 1998; 395:78–82. [PubMed: 9738501]

Hua JY, Smith SJ. Neural activity and the dynamics of central nervous system development. Nat Neurosci. 2004; 7:327–332. [PubMed: 15048120]

Kim K, Li C. Expression and regulation of an FMRFamide-related neuropeptide gene family in Caenorhabditis elegans. J Comp Neurol. 2004; 475:540–550. [PubMed: 15236235]

Klassen MP, Shen K. Wnt signaling positions neuromuscular connectivity by inhibiting synapse formation in C. elegans. Cell. 2007; 130:704–716. [PubMed: 17719547]

Klopfenstein DR, Vale RD. The lipid binding pleckstrin homology domain in UNC-104 kinesin is necessary for synaptic vesicle transport in Caenorhabditis elegans. Mol Biol Cell. 2004; 15:3729–3739. [PubMed: 15155810]

Koushika SP, Schaefer AM, Vincent R, Willis JH, Bowerman B, Nonet ML. Mutations in Caenorhabditis elegans cytoplasmic dynein components reveal specificity of neuronal retrograde cargo. J Neurosci. 2004; 24:3907–3916. [PubMed: 15102906]

Lagace DC, Benavides DR, Kansy JW, Mapelli M, Greengard P, Bibb JA, Eisch AJ. Cdk5 is essential for adult hippocampal neurogenesis. Proc Natl Acad Sci U S A. 2008; 105:18567–18571. [PubMed: 19017796]

Lai KO, Ip NY. Recent advances in understanding the roles of Cdk5 in synaptic plasticity. Biochim Biophys Acta. 2009

Lichtman JW, Colman H. Synapse elimination and indelible memory. Neuron. 2000; 25:269–278. [PubMed: 10719884]

Mahoney TR, Liu Q, Itoh T, Luo S, Hadwiger G, Vincent R, Wang ZW, Fukuda M, Nonet ML. Regulation of synaptic transmission by RAB-3 and RAB-27 in Caenorhabditis elegans. Mol Biol Cell. 2006; 17:2617–2625. [PubMed: 16571673]

Mello C, Fire A. DNA transformation. Methods Cell Biol. 1995; 48:451–482. [PubMed: 8531738]

Miyawaki A. Fluorescent proteins in a new light. Nat Biotechnol. 2004; 22:1374–1376. [PubMed: 15529159]

Niwa S, Tanaka Y, Hirokawa N. KIF1Bbeta- and KIF1A-mediated axonal transport of presynaptic regulator Rab3 occurs in a GTP-dependent manner through DENN/MADD. Nat Cell Biol. 2008; 10:1269–1279. [PubMed: 18849981]

Ou CY, Poon VY, Maeder CI, Watanabe S, Lehrman EK, Fu AK, Park M, Fu WY, Jorgensen EM, Ip NY, Shen K. Two cyclin-dependent kinase pathways are essential for polarized trafficking of presynaptic components. Cell. 2010; 141:846–858. [PubMed: 20510931]

Pack-Chung E, Kurshan PT, Dickman DK, Schwarz TL. A Drosophila kinesin required for synaptic bouton formation and synaptic vesicle transport. Nat Neurosci. 2007; 10:980–989. [PubMed: 17643120]

Puthanveettil SV, Monje FJ, Miniaci MC, Choi YB, Karl KA, Khandros E, Gawinowicz MA, Sheetz MP, Kandel ER. A new component in synaptic plasticity: upregulation of kinesin in the neurons of the gill-withdrawal reflex. Cell. 2008; 135:960–973. [PubMed: 19041756]

Ruthazer ES, Li J, Cline HT. Stabilization of axon branch dynamics by synaptic maturation. J Neurosci. 2006; 26:3594–3603. [PubMed: 16571768]

Sanes JR, Lichtman JW. Development of the vertebrate neuromuscular junction. Annu Rev Neurosci. 1999; 22:389–442. [PubMed: 10202544]

Seeburg DP, Feliu-Mojer M, Gaiottino J, Pak DT, Sheng M. Critical role of CDK5 and Polo-like kinase 2 in homeostatic synaptic plasticity during elevated activity. Neuron. 2008; 58:571–583. [PubMed: 18498738]

Trachtenberg JT, Chen BE, Knott GW, Feng G, Sanes JR, Welker E, Svoboda K. Long-term in vivo imaging of experience-dependent synaptic plasticity in adult cortex. Nature. 2002; 420:788–794. [PubMed: 12490942]

White JG, Albertson DG, Anness MA. Connectivity changes in a class of motoneurone during the development of a nematode. Nature. 1978; 271:764–766. [PubMed: 625347]

Zhang J, Herrup K. Cdk5 and the non-catalytic arrest of the neuronal cell cycle. Cell Cycle. 2008; 7:3487–3490. [PubMed: 19001851]

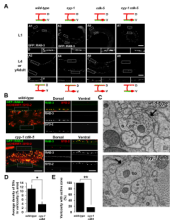

Figure 1. CYY-1 and CDK-5 Are Required for Synaptic Remodeling in DDs

(A) *Wild-type* animals expressing GFP::RAB-3 in DD motoneurons (*wyIs202*) at the stages of L1 (A1) and L4 or young adult (A2). *cyy-1* and *cdk-5* single-mutants show incomplete elimination of ventral GFP::RAB-3 puncta at the stages of L4 or young adult (A4 and A6). In *cyy-1 cdk-5* double-mutant, most of GFP::RAB-3 puncta are in the ventral processes (A8). All the single- and double-mutants exhibit wild-type localization of GFP::RAB-3 on the ventral side at the stage of L1 (A3, A5, and A7). Schematic diagrams showing phenotypes are shown above and below each image. Green dots, GFP::RAB-3; red lines, DD ventral and dorsal processes and commissures; red ovals, DD cell bodies; D, dorsal processes; V, ventral processes. Magnified images are shown for representative regions (white dotted boxes) of dorsal (D) and ventral (V) processes. Scale bars, 20 μm. See also Figures S2 and S3.

(B) Ventral GFP::RAB-3 puncta of DD neurons in *cyy-1 cdk-5* double-mutants colocalize with an active zone protein SYD-2/Liprin-α. *Wild-type* or *cyy-1 cdk-5* double-mutant animals coexpressing GFP::RAB-3 and mCHERRY::SYD-2 in DD motoneurons (*wyEx3650*) were imaged at the stages of L4 or young adult. Representative regions (white dotted boxes) are magnified on the right side. Scale bars, 20 and 10 μm for low and high magnification images, respectively.

(C) Dorsal synapses of DD neurons in *cyy-1 cdk-5* double-mutants are defective at the stage of young adult. Representative EM images of varicosities of DD in *wild-type* (upper) or *cyy-1 cdk-5* double-mutant animals (lower). Arrows, active zones.

(D and E) Average density of synaptic vesicles (SVs) in each varicosity (D) and the percentage of varicosities with active zones (E) were quantified. Error bars, standard error. Number of varicosities = 5 and 6 for *wild-type* and *cyy-1 cdk-5* double-mutant worms, respectively. * $p < 0.05$, *t-test*; **$p < 0.0001$, χ^2 test.

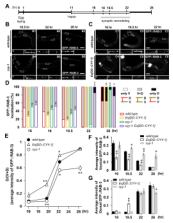

Figure 2. CYY-1 Is Required for the Completion of DD Synaptic Remodeling

(A) Schematic of experimental timeline. Experiments were performed at 25 °C. See experimental procedures for details. White box denotes the L1 stage. See also Figure S1.

(B) *cyy-1* mutants exhibit incomplete synaptic remodeling. Note that *cyy-1* mutants still have significant amount of GFP::RAB-3 in the ventral processes at 26-hr (B6). Scale bars, 20 μm.

(C) Overexpression of CYY-1 accelerates DD synaptic remodeling. Note the weak ventral GFP::RAB-3 signal at 16-, 19.5-, and 22-hr in worms overexpressing CYY-1 (C4–C6). Scale bars, 20 μm.

(D) Quantification for appearance of dorsal GFP::RAB-3 and disappearance of ventral GFP::RAB-3. The X axis indicates the time points since egg-laying. White, gray, and black indicate worms showing GFP::RAB-3 signals only in the ventral (only V), both in the ventral and dorsal (V+D), and only in the dorsal (only D) sides, respectively, regardless of their intensity. *wyEx2844* is *Ex[DD::CYY-1]* in *wild-type* background, and *wyEx2889* is *Ex[DD::CYY-1]* in *cyy-1* mutant background. *p<0.05, **p<0.005, ns, not significant relative to *wild-type*; #p<0.05, ##p<0.005, NS, not significant relative to *cyy-1*, *Fisher's exact test*. Symbols for statistics are labeled inside of the gray-filled and above the black-filled bars for the phenotypes of "V+D" and "only D", respectively.

(E, F, and G) Average intensity quantification for the ratio of dorsal to ventral plus dorsal [D/(V+D)] GFP::RAB-3 (E), for ventral GFP::RAB-3 (F), and for dorsal GFP::RAB-3 (G) from Figures 2B and 2C. Data represent means ± SEM. *p<0.05, **p<0.005 relative to *wild-type*, *student t-test*. See the Supplemental Data for n numbers. See also Figure S4.

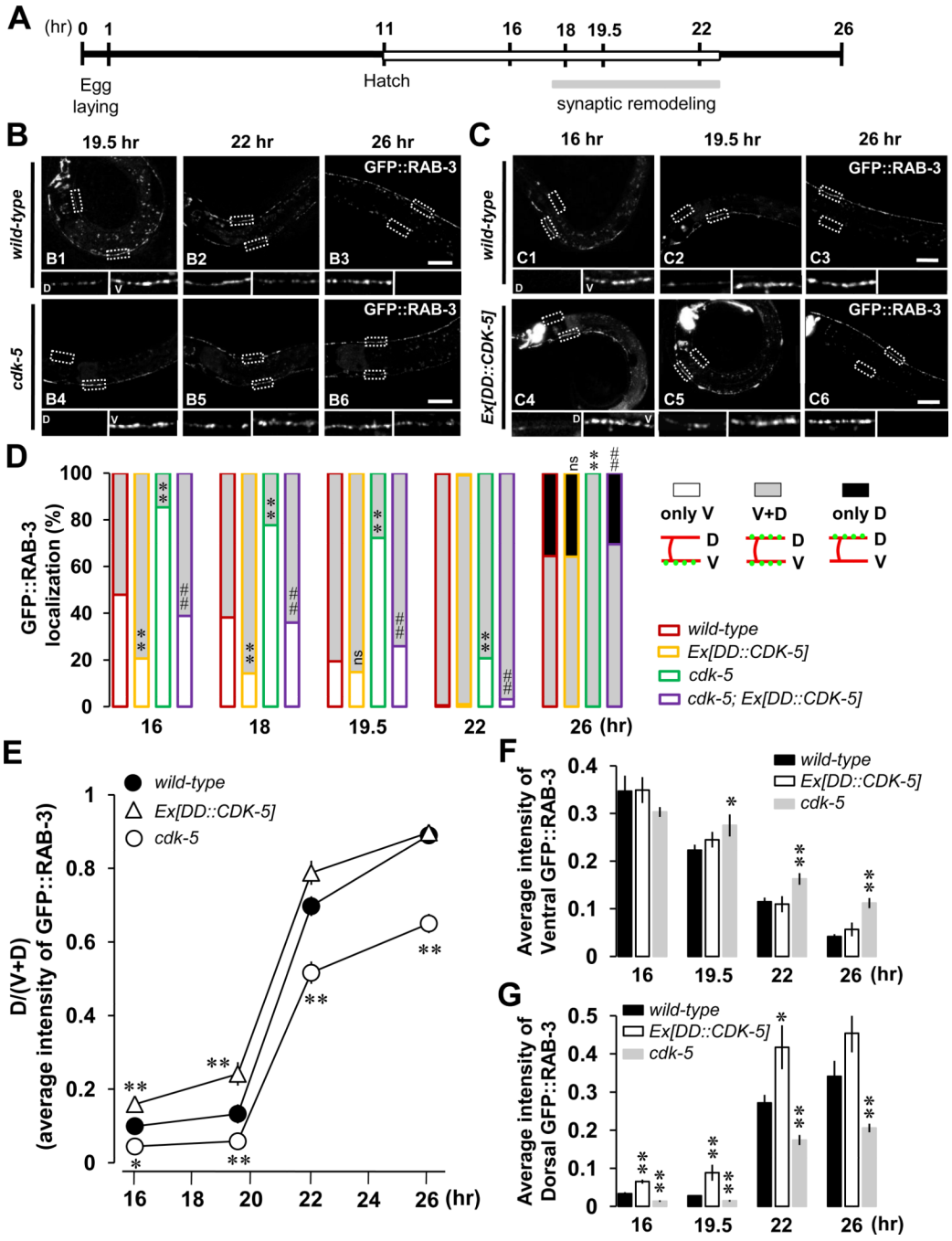

Figure 3. CDK-5 Is Required for the Completion of DD Synaptic Remodeling

(A) Schematic of experimental timeline. Experiments were performed at 25 °C. See experimental procedures for details.

(B) *cdk-5* mutants exhibit impaired synapse formation in the dorsal process and incomplete elimination of ventral synapses during DD synaptic remodeling. Note that about 80 % of *cdk-5* mutant worms do not have GFP::RAB-3 yet in the dorsal processes at 19.5-hr (B4) and still have a significant amount of GFP::RAB-3 in the ventral processes at 26-hr (B6). Scale bars, 20 μm.

(C) Overexpression of CDK-5 accelerates dorsal synapse formation during the remodeling. Note that about 80 % of worms overexpressing CDK-5 show GFP::RAB-3 puncta in the dorsal processes even at 16-hr (C4). Scale bars, 20 μm.
(D) Quantification as described in the Figure 2D legend. *p<0.05, **p<0.005, ns, not significant relative to *wild-type*; #p<0.05, ##p<0.005, NS, not significant relative to *cdk-5, Fisher's exact test*. Symbols for statistics are labeled inside of the gray-filled and above the black-filled bars for the phenotypes of "V+D" and "only D", respectively.
(E, F, and G) Average intensity quantification for the ratio of dorsal to ventral plus dorsal [D/(V+D)] GFP::RAB-3 (E), for ventral GFP::RAB-3 (F), and for dorsal GFP::RAB-3 (G) from Figures 3B and 3C. Data represent means ± SEM. *p<0.05, **p<0.005 relative to *wild-type, student t-test*. See the Supplemental Data for n numbers.

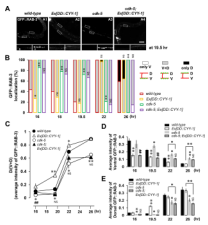

Figure 4. CYY-1 and CDK-5 Play Differential Roles During DD Synaptic Remodeling

(A) Shown are representative images at 19.5-hr time point. Scale bar, 20 μm.

(B) Quantification as described in the Figure 2D legend. *wyEx2844* is *Ex[DD::CYY-1]* in *wild-type* background, and *wyEx2889* is *Ex[DD::CYY-1]* in *cdk-5* mutant background. *p<0.05, **p<0.005, ns, not significant relative to *wild-type*; #p<0.05, ##p<0.005, NS, not significant relative to *cdk-5*, *Fisher's exact test*. Symbols for statistics are labeled inside of the gray-filled and above the black-filled bars for the phenotypes of "V+D" and "only D", respectively.

(C, D, and E) Average intensity quantification for the ratio of dorsal to ventral plus dorsal [D/(V+D)] GFP::RAB-3 (C), for ventral GFP::RAB-3 (D), and for dorsal GFP::RAB-3 (E). Data represent means ± SEM. *p<0.05, **p<0.005 relative to *wild-type* otherwise indicated; #p<0.05, ###p<0.005, NS, not significant relative to *cdk-5*, *student t-test*. See the Supplemental Data for n numbers.

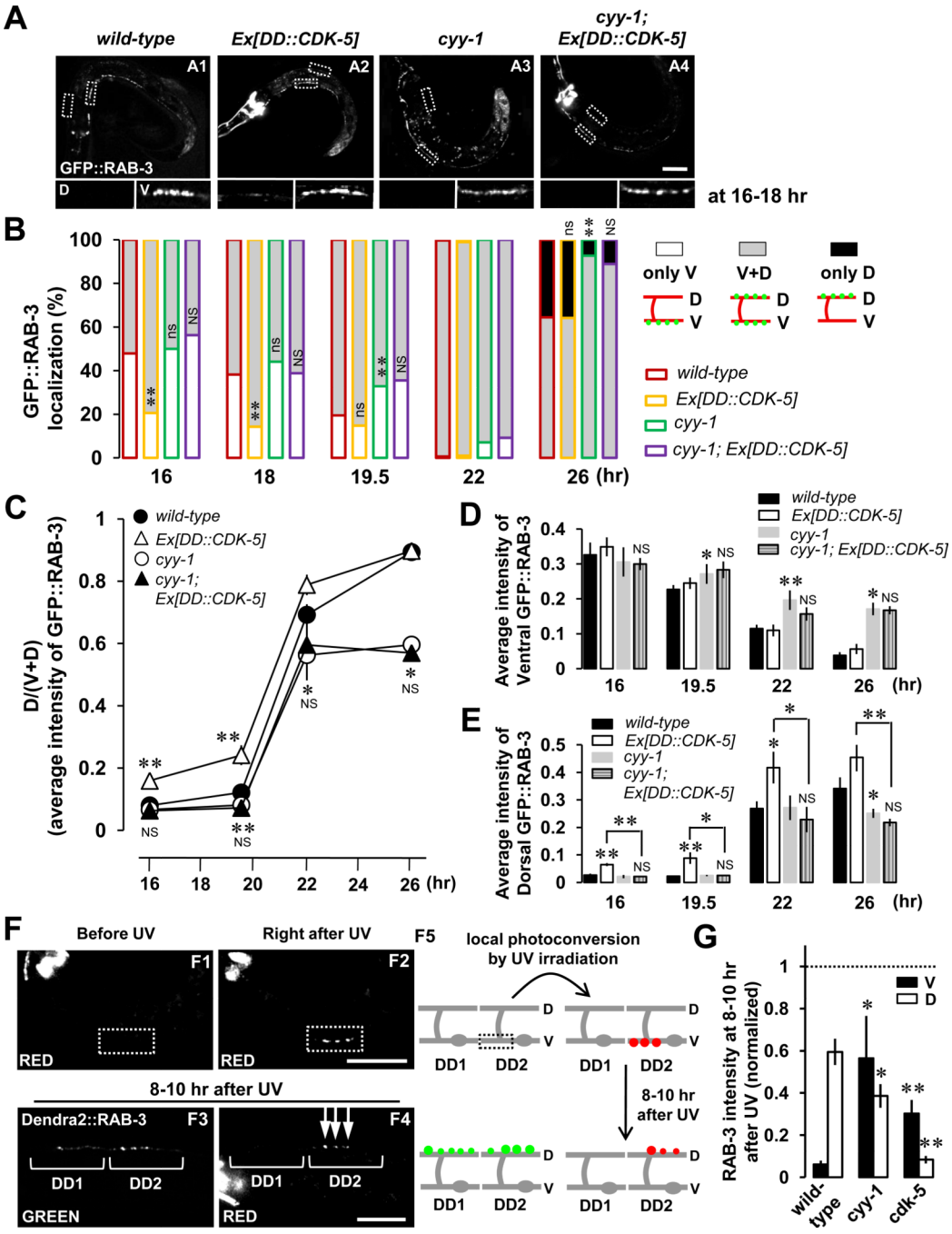

Figure 5. CYY-1 Contributes to the Function of CDK-5 to Form Dorsal Synapses During DD Synaptic Remodeling

(A) Representative images of GFP::RAB-3 in four different genotypes at 16–18-hr time-points. Scale bar, 20 μm.

(B) Quantification of the progression of remodeling in control animals as well as *cyy-1; Ex[DD::CDK-5]*. The same convention of statistical analysis was used as in the Figure 2D legend. *p<0.05, **p<0.005, ns, not significant relative to *wild-type*; #p<0.05, ##p<0.005, NS, not significant relative to *cyy-1, Fisher's exact test*. Symbols for statistics are labeled inside of the gray-filled and above the black-filled bars for the phenotypes of "V+D" and "only D", respectively.

(C, D, and E) Average intensity quantification for the ratio of dorsal to ventral plus dorsal [D/(V+D)] GFP::RAB-3 (C), for ventral GFP::RAB-3 (D), and for dorsal GFP::RAB-3 (E). Data represent means ± SEM. *p<0.05, **p<0.005 relative to *wild-type*, NS, not significant relative to *cyy-1*, *student t-test*. See the Supplemental Data for n numbers.

(F) Disassembled ventral synaptic components are reused for dorsal synapse formation during DD synaptic remodeling. Dendra2::RAB-3 in the DD2 ventral process was locally activated by UV irradiation before the start of DD remodeling (F1, white dotted box). Right after UV irradiation (30 mW, 20 sec), the green fluorescence from Dendra2::RAB-3 is photoconverted to red fluorescence (F2, white dotted box). Photoconverted red fluorescent Dendra2::RAB-3 was examined in the dorsal processes 8–10 hr after UV irradiation (around 26-hr time point, F4, arrows). Note that as a control, DD1 neuron, that has never been photoconverted by UV, exhibits only green (F3), but not red (F4) fluorescent Dendra2::RAB-3 puncta in the dorsal process 8–10 hr after UV irradiation. Schematic diagrams were illustrated in F5. Scale bars, 20 μm.

(G) Transportation of photoconverted ventral RAB-3 to the dorsal process is inhibited in *cyy-1* and *cdk-5* mutants. The integrated intensity of photoconverted Dendra2::RAB-3 at 8–10 hr after UV irradiation (F4) was normalized to the integrated intensity of photoconverted Dendra2::RAB-3 right after UV irradiation (F2) in *wild-type*, *cyy-1*, or *cdk-5* mutant worms. Note that 59% of photoconverted ventral RAB-3 are reused for new synapse formation in the dorsal process (*wild-type*). Also, note that 95% of photoconverted RAB-3 fluorescence are recovered at 8–10 hr after UV when the fluorescence in the ventral (black) and dorsal process (white) was added in *cyy-1* mutants. Note that only 8.4% of photoconverted ventral RAB-3 are transported to the dorsal process in *cdk-5* mutants. n (from left to right)= 10, 5, 6. *p<0.05, **p<0.005 relative to *wild-type*, *student t-test*.

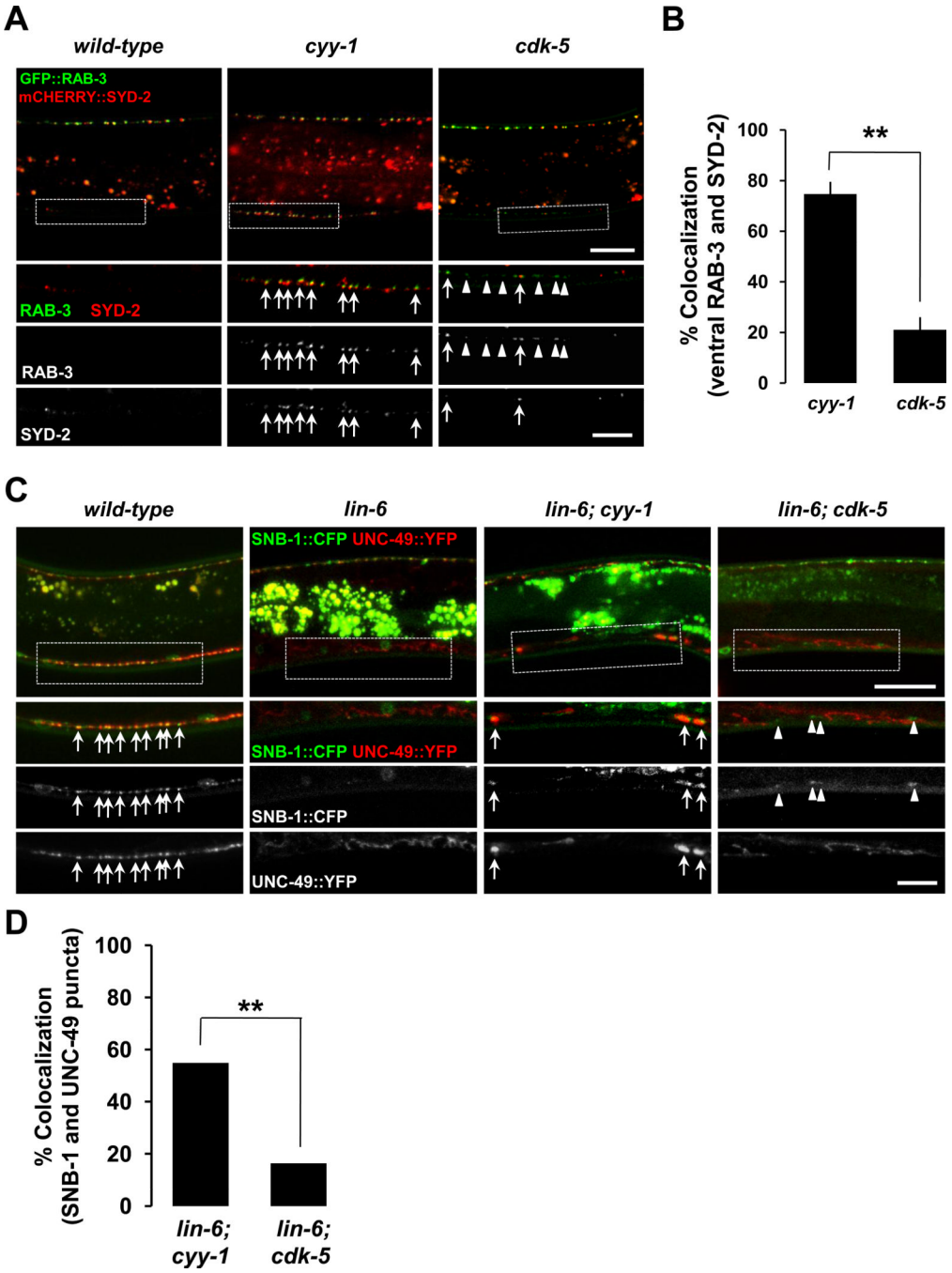

Figure 6. Ectopic Ventral RAB-3 or SNB-1 Puncta in *cyy-1*, But Not in *cdk-5* Mutants, Colocalize with Active Zone SYD-2 Proteins and Postsynaptic UNC-49/GABA Receptors

(A) GFP::RAB-3 and mCHERRY::SYD-2 are coexpressed in *wild-type* (left), *cyy-1* (middle), or *cdk-5* mutant background (right). Note the high degree of colocalization of ventral GFP::RAB-3 with mCHERRY::SYD-2 in *cyy-1*, but not *cdk-5* mutants. Ventral regions are magnified (white dotted boxes). Arrows, ventral RAB-3 overlapping with SYD-2; Arrowheads, ventral RAB-3 non-overlapping with SYD-2. Imaged at the stage of L4. Scale bars, 20 and 10 μm for low and high magnification images, respectively.

(B) The percentage of ventral GFP::RAB-3 puncta overlapping with mCHERRY::SYD-2 was quantified. Data represent means ± SEM. n=196 and 183 ventral GFP::RAB-3 puncta from 14 and 11 worms for *cyy-1* and *cdk-5*, respectively. **p<0.0001; *Student t-test*.
(C) Ectopic ventral SNB-1/synaptobrevin puncta of DD neurons in *cyy-1* mutants colocalize with UNC-49/GABA receptors of the ventral body muscle. *krIs1* strain (Gally and Bessereau, 2003) was used to label presynaptic SNB-1/synaptobrevin and postsynaptic UNC-49/GABA receptors simultaneously in *wild-type*, *lin-6*, *lin-6; cyy-1*, or *lin-6; cdk-5* mutant background. Note the high degree of colocalization of ventral SNB-1::CFP with UNC-49::YFP in *lin-6; cyy-1*, but not *lin-6; cdk-5* mutants. Ventral regions are magnified (white dotted boxes). Arrows, ventral SNB-1 overlapping with UNC-49 puncta; Arrowheads, ventral SNB-1 non-overlapping with UNC-49 signals. Imaged at the stages of L3 to young Adult. Scale bars, 20 and 10 μm for low and high magnification images, respectively.
(D) The percentage of ventral SNB-1::CFP puncta overlapping with UNC-49::YFP was quantified. n=82 and 61 ventral SNB-1::CFP puncta from 17 and 15 worms for *lin-6; cyy-1* and *lin-6; cdk-5*, respectively. **p<0.0001; *Fisher's exact test*.

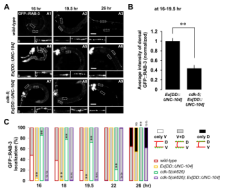

Figure 7. CDK-5 and UNC-104/Kinesin3 Act Together To Form New Dorsal Synapses During DD Remodeling

(A and B) UNC-104-mediated dorsal synapse formation is inhibited in the absence of CDK-5. Note the much reduced GFP::RAB-3 intensity in the dorsal processes in the absence of CDK-5 (D inserts of A7 and A8) compared to that in the presence of CDK-5 (D inserts of A4 and A5). D, dorsal processes; V, ventral processes; Scale bars, 20 μm. Average intensity of dorsal GFP::RAB-3 was quantified during 16~19.5-hr time points (B). Data represent means ± SEM. n (from left to right)= 26, 16. **p<0.0005 compared to *wild-type*; Student *t-test*.

(C) Quantification as described in the Figure 2D legend. *p<0.05, **p<0.005, ns, not significant relative to *wild-type*; #p<0.05, ##p<0.005, NS, not significant relative to *cdk-5*, *Fisher's exact test*. Symbols for statistics are labeled inside of the gray-filled and above the black-filled bars for the phenotypes of "V+D" and "only D", respectively. See the Supplemental Data for n numbers. See also Figure S6.

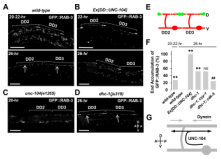

Figure 8. UNC-104 and Dynein Motor Proteins Act Temporally To Properly Pattern the Synapses Along the Dorsal Process During DD Synaptic Remodeling

(A) UNC-104 transports synaptic vesicles toward both anterior and posterior ends of dorsal processes during DD synaptic remodeling. In *wild-type* worms, synaptic vesicles labeled by GFP::RAB-3 are transported to the both anterior and posterior ends of dorsal processes (20–22-hr, upper), and then redistribute evenly along the processes (26-hr, lower) during the remodeling.

(B and C) Overexpression of UNC-104 in DDs directs GFP::RAB-3 accumulated in the anterior and posterior ends of dorsal processes (B) during the remodeling. But, in *unc-104(e1265)* mutants, the transport of GFP::RAB-3 to the dorsal process is completely blocked (C).

(D) In *dhc-1(js319)* mutants, GFP::RAB-3 accumulates in both anterior and posterior ends of dorsal process even at 26-hr time point. Arrows indicate the location of commissures. Brackets mark the length of dorsal axons of individual DD neurons. Scale bars, 20 μm.

(E) Schematic diagram for both anterior and posterior ends accumulation phenotype that is examined in (A, 22-hr), (B), and (D), and is quantified in (F).

(F) Quantification of the phenotype for the end accumulation of GFP::RAB-3 as in (E). n (from left to right)=136, 99, 70, 106, 64, 57. **<0.0001 compared to *wild-type*, 26-hr, ##<0.001 compared to *dhc-1*, 26-hr, *Fisher's exact test*.

(G) Schematic diagram for the roles of two motor proteins, UNC-104 and Dynein for synapse formation during DD synaptic remodeling. Straight gray lines, dorsal and ventral processes; curved gray line, commissure; gray oval, cell body. Transport directions are indicated by black and gray arrows for UNC-104 and Dynein, respectively.